Demystifying Transmission Lines: What are They? Why are They Useful?

Purpose of This Note

This application note discusses theory and practice of transmission lines. It outlines the necessity of transmission lines for modeling porous electrodes in Electrochemical Impedance Spectroscopy (EIS) and describes different kinds of models.

Several practical examples of different electrochemical energy storage and generation devices give suggestions how to evaluate such EIS spectra with Gamry's Echem Analyst.

Introduction

The classical electrochemical interface can be described by a plane electron-conducting electrode and an ion-conducting electrolyte. Electrochemical reactions occur on the surface of the electrode.

The electrochemical behavior of this interface can be described by different models. One of the simplest and most common models is the so-called Randles model shown in Figure 1.
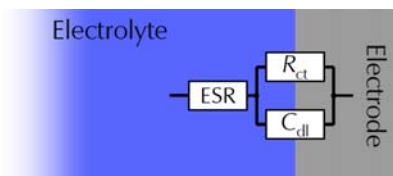
Figure 1 – Diagram of a simplified Randles model describing the electrochemical interface on plane electrodes.

The "equivalent series resistance" (ESR) represents the sum of resistances from the electrode, electrolyte, and electrical contacts. It is in series to a parallel connection of charge-transfer resistance R_{ct} and double layer capacitance C_{dl}.

R_{ct} represents all Faradaic reactions that occur on the electrode's surface. These reactions can be reversible and irreversible. In contrast, C_{dl} describes non-Faradaic charge storage mechanisms. It is often replaced by a "constant phase element" for non-ideal assumptions.

This model is good for approximations and for describing electrochemical interfaces of plane electrodes. But it poorly describes the effect of porous electrodes that are used in most electrochemical cells.

Porous Electrodes

To increase performance, energy storage and generation devices such as electrochemical capacitors (ECs), fuel cells, or dye-sensitized solar cells (DSCs) use highly porous electrodes. These electrodes exhibit a very high surface compared to volume or weight. For example, ECs can have specific electrode surfaces of 1000 m^2/g and more.

Electrodes that are using highly porous materials can be differentiated into two parts – the base electrode and the porous electrode. The base electrode is generally an insulated and inactive metal foil where the active material is fixed on. Figure 2 shows a schematic setup.
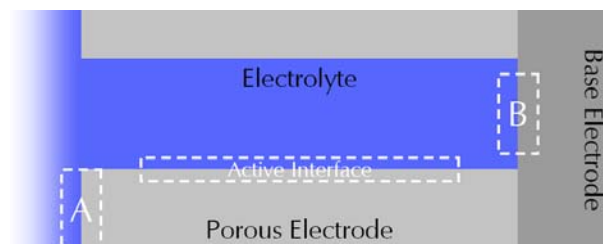
Figure 2 – Classification of regions for a porous electrode interface.

Compared to plane electrodes (see Figure 1), reactions occur directly on the surface of the electrode. In contrast, the reaction velocity within the pore of porous electrodes is limited. The access to the active interface for ions is hindered due to the small inner volume of the pores. Hence electrochemical reactions gradually delay the farther

ions penetrate into the pore. This step becomes the dominating part.

Due to these restrictions on the electrochemical reactivity, the porous electrode has to be divided into three regions. These interfaces are marked "A", "B", and "Active Interface" (see Figure 2).

Region "A" represents the interface between the outer surface of the porous electrode and the electrolyte. Region "B" describes interactions between electrolyte and base electrode.

The most reactive parts itself is within the pore. This region is called "Active Interface". It describes the interactions between active material of the porous electrode and electrolyte.

To investigate all these phenomena, EIS is the most common technique in research. It allows studying reaction mechanisms of electrochemical systems in a generally non-destructive way.

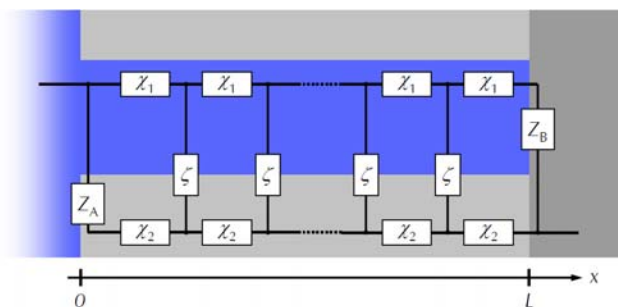For better understanding, different fit models can be used to estimate electrode and electrolyte parameters. In the following sections, different models will be introduced and explained by means of measurements on real cells. To follow the content of this application note, basic knowledge of EIS and modeling equivalent circuits is assumed.

Figure 3 – Scheme of a generic transmission line model.

L is the length of the transmission line or the depth of the pore respectively. The two interfaces "A" and "B" are represented by impedances $Z_A(x = 0)$ on the outer surface of the pore and $Z_B(x = L)$ on the base electrode at the end of the pore. Along the pore, the transmission line is represented by repeating impedance elements.

χ_1 is the impedance of the electrolyte within the pore. Note that this impedance is different to the bulk electrolyte resistance that is represented as part of

$$Z = \frac{1}{\chi_1 + \chi_2}\left[\lambda(\chi_1 + \chi_2)S_\lambda + (Z_A + Z_B)C_\lambda + \frac{Z_A Z_B S_\lambda}{\lambda(\chi_1 + \chi_2)}\right]^{-1} \cdot \left[L\lambda\chi_1\chi_2(\chi_1 + \chi_2)S_\lambda + \chi_1(\lambda\chi_1 S_\lambda + L\chi_2 C_\lambda)Z_A\right.$$

$$\left. + \chi_2(\lambda\chi_2 S_\lambda + L\chi_1 C_\lambda)Z_B + \left(2\chi_1\chi_2 + (\chi_1^2 + \chi_2^2)C_\lambda + \frac{L}{\lambda}\chi_1\chi_2 S_\lambda\right)\frac{Z_A Z_B}{\chi_1 + \chi_2}\right] \qquad \text{Eq 1}$$

with $\lambda = [\zeta/(\chi_1 + \chi_2)]^{1/2}$, $C_\lambda = \cosh(L/\lambda)$, and $S_\lambda = \sinh(L/\lambda)$.

the ESR. χ_2 is the impedance of the porous electrode's solid phase. Both parameters describe the ohmic drop between $0<x<L$. ζ describes the impedance at the "Active Interface" region shown in Figure 2.

Juan Bisquert[1] calculated the impedance Z for a general transmission line model (see equation 1). This equation is the basis for modeling transmission lines for EIS spectra. For his calculations he assumed that χ_1, χ_2, and ζ are independent on their position ($0<x<L$) within the pore. Hence they can be treated as homogenously distributed.

In practice, knowing the pore depth L allows to determine important parameters such as the conductivity and diffusion coefficients from the impedance fit results. However, this would go beyond the scope of this application note. Please see cited literature for detailed information.

> If you need basic information on EIS and circuit modeling, see Gamry's Application Notes section at **www.gamry.com**:
>
> **Basics of Electrochemical Impedance Spectroscopy**
>
> **Equivalent Circuit Modeling in EIS**

Transmission lines

The stepwise flux of ions within a pore can be described by a so-called transmission line. Figure 3 shows a model in its generic form. The model consists of several parallel and serially connected elements. It is used to describe the different regions shown in Figure 2.

Fitting transmission lines in the Echem Analyst

Gamry's Echem Analyst contains several pre-built EIS models including different transmission line models that can be used instantly or modified.

In addition, the model editor enables building own EIS models. A variety of most common elements can be interconnected to describe different electrochemical systems.

> For more information implementing and modifying circuit models, see Gamry's Application Notes section at **www.gamry.com**:
>
> **User-Defined Components in EIS Circuit Modeling**

For adjusting and calculating model parameters, the Echem Analyst offers two different algorithms. A Simplex algorithm and a Levenberg-Marquardt algorithm calculate the impedance to find adequate fit-parameters. First one also has an Auto-Fit function for easier finding start parameter. The latter one is faster but requires partial derivates of the impedance for each parameter.

The next sections describe all pre-built transmission line models in the Echem Analyst.

"Unified" model

The "*Unified*" model can be used for testing different boundary conditions and limitations regarding the electrode. Limiting cases of transmission lines can be easily achieved by adjusting appropriate elements to be zero or very large.

The transmission line model "*Unified*" is shown in Figure 4. In addition, a resistor (not shown) is in series to the model. It represents the ESR.

This model uses only the Simplex algorithm as its derivates would be computational and algebraic prohibitive to calculate. In total, eleven parameters can be modified and calculated.
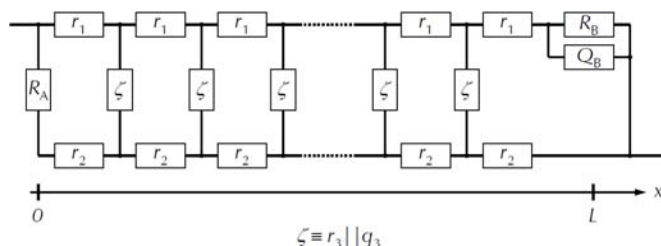
Figure 4 – Scheme of the transmission line model "*Unified*". For details, see text.

Compared to the generic form of Figure 3, single and repeating impedances are replaced by specific elements:

- $\chi_1 \equiv r_1$
- $\chi_2 \equiv r_2$
- $\zeta \equiv r_3 \| q_3$
- $Z_A \equiv R_A$
- $Z_B \equiv R_B \| Q_B$

> Note that lowercase letters are used for repeating elements and capital letters for single elements. Resistors will be represented with an R (or r) and constant phase elements will use the letter Q (or q).
>
> The symbol "$\|$" will be used to indicate a parallel combination of components.

Z_B and ζ are both represented as parallel combination of resistor and constant phase element. The resistor describes charge-transfer reactions at the interface. The constant phase element summarizes all polarization effects. In an ideal case, it can be treated as capacitor. However, a constant phase element addresses also non-ideal capacitances resulting from inhomogeneities of porous electrodes.

All other components in the "*Unified*" model – Z_A, χ_1, and χ_2 – are represented by simple resistors.

"Bisquert Open" and "Bisquert Short"

Figure 5 shows two transmission line models which describe limiting cases of the general transmission line model. Both were originally developed by Bisquert[2] to describe diffusion and recombination processes.

Model a) is called "*Bisquert Open*" (BTO) and b) is called "*Bisquert Short*" (BTS). In the Analyst, an additional resistor is in series to the model. It represents the ESR and is not shown in Figure 5.
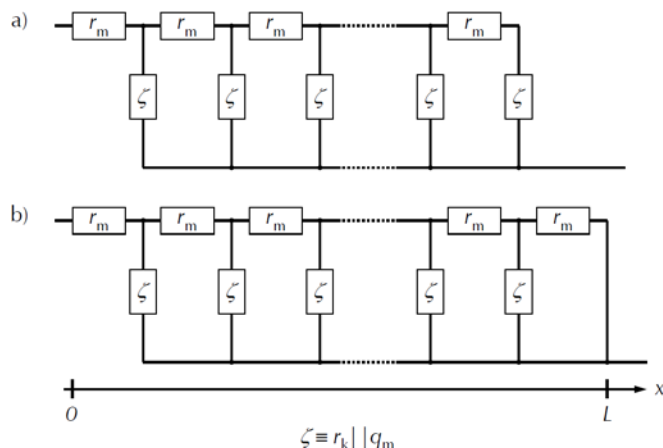
Figure 5 – Two specific cases of transmission line models. (a) Bisquert Open (BTO) and (b) Bisquert Short (BTS). For details, see text.

The boundary conditions for both models are:

- $\chi_1 \equiv r_m$ - $\chi_2 \equiv 0$ - $\zeta \equiv r_k \| q_m$
- $Z_A \equiv \infty$
- $Z_B \equiv \infty$ (BTO)   - $Z_B \equiv 0$ (BTS)

In both models it is assumed that the conductivity of one resistive trail is much larger than the other one. Hence the impedance of the electrode's solid phase χ_2 can be set to zero. Only the electrolyte resistance r_m within the pore is considered.

Similar to the "*Unified*" model, impedance ζ of the active interface is a parallel circuit of resistor and constant phase element. Both represent Faradaic and capacitive non-Faradaic reactions respectively.

Impedance Z_A is set to infinite (open circuited). This means in practice that electrochemical reactions do not occur on the surface of the porous electrode. Only reactions within the pore are going to be considered. Z_A can be completely neglected at the fitting process.

The difference in both models is impedance Z_B. At the "*Bisquert Open*" model, Z_B is also set to infinite. The system is defined by "*reflecting boundary conditions*". This means that the base electrode is completely insulating and no reactions (Faradaic or non-Faradaic) occur on its surface.

> **Note:** "R*eflecting boundary condition*" does not mean capacitive behavior. While capacitors exhibit infinite impedance only at frequencies near zero, Z_B is infinite for all frequencies.

In contrast, Z_B is zero for the "*Bisquert Short*" model. This system is defined by "*absorbing boundary conditions*". Hence the substrate's surface is not entirely insulated and also interacts with the electrolyte. This would short-circuit the porous film.

Bisquert[2] calculated for both models the total impedance. The results are shown in Equation 2 and 3.

$$Z_{BTO} = \sqrt{\zeta \cdot \chi_1} \coth\left(L\sqrt{\frac{\chi_1}{\zeta}}\right) \qquad \text{Eq 2}$$

$$Z_{BTS} = \sqrt{\zeta \cdot \chi_1} \tanh\left(L\sqrt{\frac{\chi_1}{\zeta}}\right) \qquad \text{Eq 3}$$

Applications

Electrochemical systems can be very different. Electrochemical capacitors base on highly reversible non-Faradaic charge separation mechanisms while DSCs base on reversible redox reactions.

In addition, if limitations of electrochemical systems are exceeded, underlying electrochemical mechanisms can change drastically. Non-reversible Faradaic reactions can occur which can lead to severe damages of the cell.

The next sections apply the prior discussed about transmission lines on practical examples.

Electrochemical capacitors

High-power electrochemical capacitors are developed for a number of applications. These include uninterruptible power supplies, lasers, and power electronics for electric and hybrid vehicles among others. They provide a very high capacitance in a relatively small volume and weight.

Figure 6 shows the Bode diagram of a potentiostatic EIS test on a 5 F electric double layer capacitor (EDLC) from Nesscap. A DC voltage of 0 V with an AC voltage of 1 mV$_{rms}$ were applied to the capacitor. The frequency range varied from 100 kHz to 5 mHz.
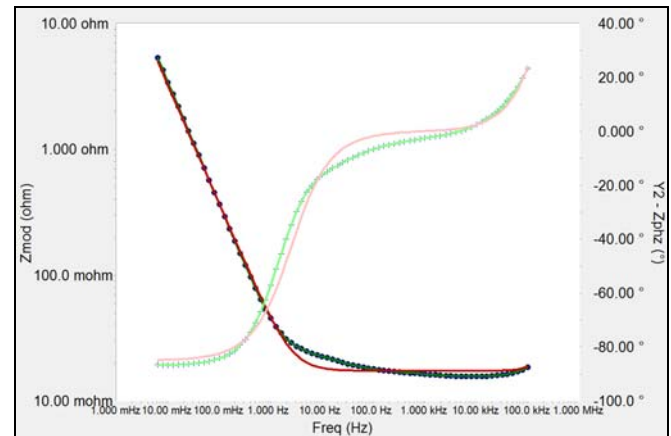
Figure 6 – Bode diagram of a potentiostatic EIS test on a 5 F EDLC (●). (●) *R*-CPE model, (●) modified "*Bisquert Open*" model. (●) magnitude, (+) phase. For details, see text.

In addition, two different fits of models are shown – a *R*-CPE model (red curve) and a modified "*Bisquert Open*" model (green curve). An additional inductance (L_1) was added to both models and is in series to the ESR. A detailed setup is shown in Figure 7.
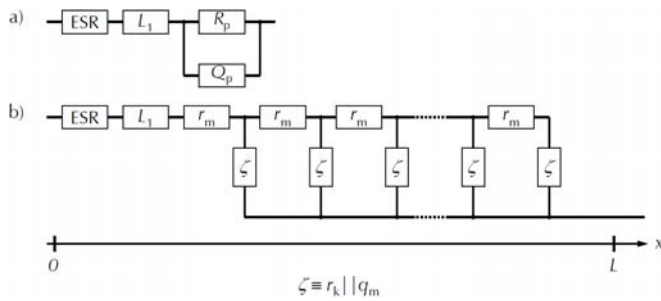
Figure 7 – Two models that are used to fit the capacitor data that are shown in Figure 6. (a) R-CPE model, (b) modified "*Bisquert Open*" model.

Model a) is an extended version of a Randles model shown in Figure 1. The double layer capacitance is replaced by a constant phase element Q_p to simulate non-ideal electrode behaviors. Model b) is a modified "*Bisquert Open*" model.

The very simple R-CPE model (red curve) shows only very poor agreement with the EIS spectrum of Figure 6. Especially at frequencies above 1 Hz, the fit starts to differ from the measured spectrum. In this region the transition from resistive to capacitive behavior occurs. The phase angle changes from nearly 0° to -90°. At very high frequencies, inductance is the dominating part showing a positive phase angle.

In contrast, the modified "*Bisquert Open*" model (green curve) overlaps nearly perfect with the capacitor's spectrum in all frequency regions. It models very well the incremental decrease of the impedance and increase of the phase angle at frequencies above 1 Hz.

Table 1 lists up fit-parameters for the modified "*Bisquert Open*" model. The pore depth L and resistance r_k are locked. Both columns are highlighted in gray. As no Faradaic reactions are expected on the active interface of the EDLC, r_k was set to a very high value.

> For adequate results, the value of L should be decided prior to the fitting and locked to a particular value. For this application note L is assumed to be dimensionless to keep the discussion straightforward.

ESR [mΩ]	L	r_m [mΩ]	r_k [Ω]	Y_m [S·s$^\alpha$]	α	L_1 [nH]
15.6	1.0	22.1	10^{35}	4.346	0.975	12.5

**Table 1** – Fit results for a 5 F EDLC using a modified "*Bisquert Open*" model.

> Note that Y_m and the dimensionless exponent α describe the constant phase element. Y_m has the unit S·s$^\alpha$ (siemens times second to the power of α).
>
> For α = 1, Y_m has the unit Farad (F) and represents an ideal capacitor. In contrast, if α = 0, Y_m is the reciprocal of a resistor with the unit S = Ω^{-1}.

Dye-sensitized solar cells

Dye-Sensitized solar cells are another application where transmission line models are regularly employed. DSCs are solar cells that utilize organic or organometallic dye molecules. They are adsorbed on mesoporous TiO$_2$ to absorb light efficiently. Excited electrons are then extracted out through the TiO$_2$.

Figure 8 shows an impedance spectrum of a DSC using porous TiO$_2$ and a liquid electrolyte. It was recorded in potentiostatic EIS mode with zero DC voltage and an AC voltage of 10 mV$_{rms}$. The frequency range ranged between 10 kHz and 70 mHz.
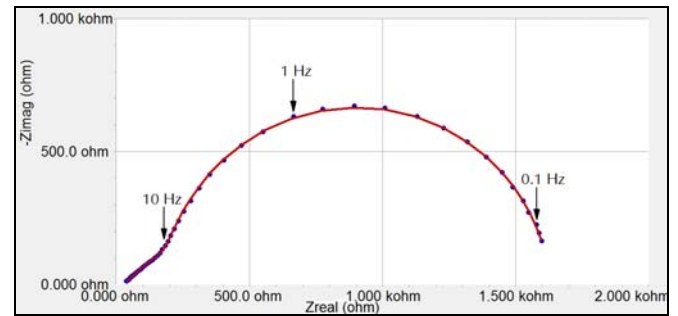
Figure 8 – Nyquist diagram of a potentiostatic EIS test on a DSC (●). (●) "*Bisquert Open*" model. For details, see text.

The Nyquist plot shows at higher frequencies a characteristic linear shape in the Nyquist diagram with a slope of about -1. This region – up to about 10 Hz – represents the transmission line. At lower frequencies the curve has the shape of a half circle representing Faradaic reactions on the electrodes surface.

The spectrum was modeled using a "Bisquert Open" model with an ESR in series. It fits nearly perfect over the entire frequency range. The fit results are summarized in Table 2. The pore depth L was again locked.

| ESR [mΩ]	L	r_m [Ω]	r_k [Ω]	Y_m [S·s$^\alpha$]	α
26.27	1.0	469.2	1452	1.84·10^{-4}	0.94

Table 2 – Fit results for a DSC using a "*Bisquert Open*" model in series with an ESR.

Note that in contrast to EDLCs (see prior section), resistance r_k is now much smaller due to Faradaic reactions occurring on the active material. The constant phase element (Y_m, α) which represents the capacitance of the system is much smaller compared to the EDLC.

In certain types of DSCs, organic hole conductors are used instead of a liquid electrolyte. Region "B", the interface between ionic conductor and base electrode, is no more completely insulating and reactions can occur.

Fabregat-Santiago et al.[4] developed a model to fit this type of DSCs. The basic model is shown in Figure 9.

$$\zeta \equiv r_3 \| q_3$$
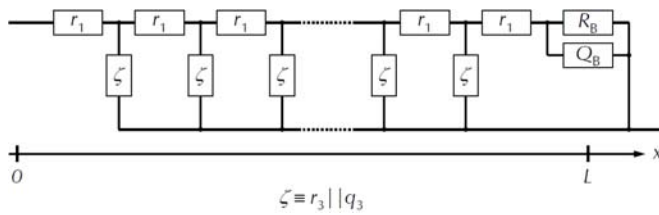
Figure 9 – Scheme of a transmission line model to describe TiO$_2$/organic hole conductor DSCs. For details, see text.

The "*Unified*" model enables the possibility to adjust appropriate parameters and to model different cell conditions. Single parameters can be individually adapted.

In this particular case, the impedance on the outer surface of the electrode's pore is open circuited. This can be simulated with a very high value for R_A. The impedance of the conducting electrode material is neglected and can be set to zero ($r_2 = 0$).

Computational simulations of Nyquist plots for this type of DSCs are shown in Figure 10. It shows different spectra for increasing reaction resistances R_B on the base electrode/electrolyte interface.
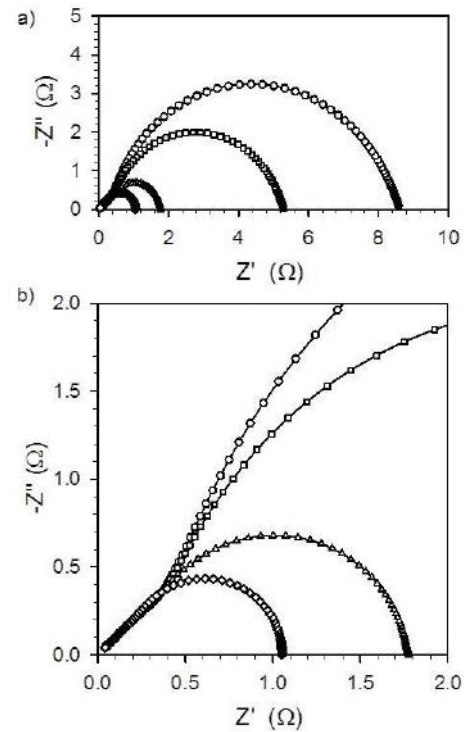
Figure 10 – a) Simulated data for the circuit depicted in Figure 9 with different reaction resistances R_B. b) Segment of the spectra. ($\Diamond$) R_B = 0.1 Ω, ($\triangle$) R_B = 1 Ω, ($\square$) R_B = 10 Ω, ($\bigcirc$) R_B = 100 Ω. For details, see text.

The spectrum of this specific case looks similar to the Nyquist plot in Figure 8. With increasing reaction resistance R_B the width of the half circle is increasing.

However, the underlying reaction mechanism is different as the base electrode is not completely insulating ("*reflecting boundary conditions*"). Electrochemical reactions (Faradaic and non-Faradaic) can occur on the base electrode.

Table 3 lists up all parameters that were used to generate the spectra of Figure 10. R_A, R_B, r_2, and the pore depth L were locked during fitting and are highlighted in gray.

R_B [Ω]	0.1	1	10	100
L	10^{-6}	10^{-6}	10^{-6}	10^{-6}
R_A [Ω]	10^{35}	10^{35}	10^{35}	10^{35}
r_1 [Ω]	10^6	10^6	10^6	10^6
r_2 [Ω]	0	0	0	0
r_3 [Ω]	$9.2 \cdot 10^{-6}$	$9.1 \cdot 10^{-6}$	$9.1 \cdot 10^{-6}$	$9.0 \cdot 10^{-6}$
Y_{o3} [S·s$^\alpha$]	$5.01 \cdot 10^3$	$5.00 \cdot 10^3$	$5.02 \cdot 10^3$	$5.00 \cdot 10^3$
α_3	1	1	1	1
Y_{oB} [S·s$^\alpha$]	$9.4 \cdot 10^{-3}$	0.01	0.01	0.01

α_B	0.717	0.700	0.699	0.700

Table 3 – Fit results for a TiO$_2$/organic hole conductor DSC using a modifed "Unified"model shown in Figure 9. Spectra were simulated with four different values of R_B (0.1 Ω, 1 Ω, 10 Ω, 100 Ω). For details, see text.

Conclusion

Porous electrodes are regularly utilized for applications where high surface areas are beneficial. Impedance spectroscopy on porous materials regularly results in data that can not be modeled with standard circuit components. Hence transmission lines are required due to the distributed nature of the interfacial impedance throughout the pore.

Theories of different models that are used in literature and included in Gamry's Echem Analyst are discussed. By means of examples on different energy storage and generation devices, utilization of the Echem Analyst and evaluation of transmission lines are shown.

Acknowledgements

Literature

[1] Bisquert, J., *Phys. Chem. Chem. Phys.*, 2, pp. 4185-4192, **2000**.
[2] Bisquert, J., *J. Phys. Chem. B*, 106, pp. 325-333, **2002**.
[3] Wang, Q.; Moser, J.-E.; Grätzel, M., *J. Phys. Chem. B*, 109, pp. 14945-19453, **2005**.
[4] Fabregat-Santiago, F.; Bisquert, J.; Garcia-Belmonte, G.; Boschloo, G.; Hagfeldt, A., *Sol. Ener. Mat. & Sol. Cells,* 87, pp. 117-131, **2005**.